

TH-UWB RECEIVER BASED ON TWO PDFS APPROXIMATION IN MULTIUSER SYSTEMS

Wang Chen^{1, 2}, Qiang Gao^{1, *}, Huagang Xiong¹, Li Fei¹, and Qiong Li²

¹School of Electronic and Information Engineering, Beihang University, Xueyuan Road No. 37, Haidian District, Beijing 100191, P. R. China

²State Key Laboratory of Wireless Mobile Communications (CATT), Xueyuan Road No. 40, Haidian District, Beijing 100191, P. R. China

Abstract—As the distribution of the multiuser interference plus noise in time-hopping ultrawide bandwidth (TH-UWB) systems can not be reliably approximated by Gaussian probability density function (PDF), the bit error rate (BER) performance of the conventional matched filter receiver in TH-UWB multiuser systems degrades. In this paper we study a novel TH-UWB receiver based on two PDFs approximating the distribution of the multiuser interference plus noise. Firstly we investigate the difference between the distribution of the multiuser interference plus noise when the received pulse is collided by interfering pulses and that when it is not. Then two PDFs are developed to approximate the distribution of multiuser interference plus noise in these two cases respectively instead of using one PDF for both cases as done in other research works. Based on these two PDFs, a new detection scheme of TH-UWB receiver is proposed. The results show that BER performance of the proposed receiver is improved by 50% or more as compared to the conventional matched filter receiver, blinking receiver, Gaussian mixture receiver and p-order receiver using simulations.

1. INTRODUCTION

Ultrawide bandwidth (UWB) wireless communication technology with merits such as high-speed transmission, low-cost transceiver circuitry and material penetration, has attracted a great deal of attention among researchers over the past few years [1–7]. In a multiuser UWB

Received 27 December 2012, Accepted 12 February 2013, Scheduled 13 February 2013

* Corresponding author: Qiang Gao (gaoqiang@buaa.edu.cn).

wireless communication system, a sequence of sub-nanosecond duration pulses are transmitted with information inserted in the polarity or the location of these pulses and an additional pseudorandom time shift is added to each pulse starting point to allow different users to share the same channel [8]. This multiple access scheme is known as time hopping (TH) method [9]. It has been shown that in TH-UWB multiuser systems the bit error rate (BER) performance of the conventional matched filter (CMF) receiver, the optimal receiver when only additive Gaussian noise is presented in the channel, is significantly degraded by the multiuser interference [10]. The CMF receiver is no longer the optimal receiver for TH-UWB systems because the multiuser interference plus noise, which will be referred to as total disturbance hereafter, is not reliably Gaussian distributed [11].

Several alternative receivers are proposed based on better models for the distribution of the total disturbance than the Gaussian approximation. The soft-limiting receiver based on Laplace probability density function (PDF) [10], GM receiver based on Gaussian mixture PDF [12] and p-order receiver based on generalized Gaussian PDF [13] are proposed and they are shown to achieve better BER performance than the CMF receiver. Instead of introducing a better model for the distribution approximation of the total disturbance the blinking receiver proposed in [14] discards the received pulses when they are collided by interfering pulses. It is shown that the blinking receiver can achieve better BER performance than the CMF receiver in the case of strong interfering signals. In [15] an optimal receiver for single user detection in TH-UWB systems is introduced using the maximum a posteriori (MAP) receiver design rule based on an exact mathematical model.

In TH-UWB communication systems, the multiuser interference (MUI) is provoked by pulse collisions [16, 17]. The distribution of the total disturbance which contains Gaussian noise and MUI when the received pulse is collided by interfering pulses may be quite different from that when the received pulse is not collided since the total disturbance in this case contains only Gaussian noise. Therefore one PDF might not be well approximating the distribution of the total disturbance, in case when the received pulse is collided and also when the received pulse is not collided. In this paper we investigate the difference of the total disturbance's distribution between the two cases above and then adopt two PDFs to approximate the distribution of the total disturbance instead of using one approximating PDF for both cases [10, 12, 13]. Specifically, we use a generalized Gaussian PDF to approximate the distribution of the total disturbance when the received pulse is collided and a Gaussian PDF to approximate the distribution

of the total disturbance when the received pulse is not collided. Based on the two approximating PDFs, a new detection scheme of TH-UWB receiver is proposed which does not discard any pulse and treats the collided pulses differently from those which are not collided.

In the proposed detection scheme, the receiver should determine whether there is a collision or not and can be implemented as following. As in [18, 19], a separate control channel is pre-assigned in the system, and each user sends a beacon in this channel before it starts sending the symbols in the data channel, thus all the user know the sending instants of the symbols. Many time-of-arrival estimation techniques have been proposed for impulse-radio UWB systems [20] with which a user knows the arriving instants of the symbols transmitted by the other users. A user in the system can select its own TH sequence and exchanges it with the other users or there is a central controller which assigns and distributes TH sequences to the users. Thus each user knows the TH sequences of all the users in the system, which is the assumption also made by [14, 21, 22]. With the assumptions above, each user knows the arriving time of the pulses sent by other users, i.e., the receiver knows whether or not the pulse of the desired user is collided.

The BER performance of the proposed receiver is compared with that of the conventional matched filter receiver, blinking receiver, Gaussian mixture receiver and p-order receiver via simulations. The results show that the novel receiver can reduce the BER by 50% or more under the circumstances investigated. The BER performance of the proposed receiver is lower than that of the optimal receiver since it detects symbols based on two PDFs of multiuser interference plus noise distribution, which approximate to the exact PDF of practical UWB pulses. The complexity of the proposed receiver is the same as that of the blinking receiver since both the receivers need to determine whether the received pulse is collided or not. The proposed receiver has higher complexity compared with CMF receiver, GM receiver and p-order receiver since a separate control channel is used to determine whether the received pulse is collided or not. Compared with the optimal receiver, our receiver needs less computation resources to acquire the PDF of MUI and less memory resources to store the PDF in the receiver. Furthermore our receiver can adapt with the changing environment since the approximate PDF of MUI can be easily determined by the system parameters, which can be easily obtained when the environment is changed.

The remainder of this paper is organized as follows. In Section 2, the TH-UWB system model considered is described. In Section 3, we investigate the distribution difference of the total disturbance and the

two PDFs for distribution approximation of the total disturbance are developed. Section 4 is devoted to describing the proposed detection scheme. In Section 5, simulation results of the BER performance of the novel receiver and other receivers are presented and discussed. Section 6 concludes this paper.

2. SYSTEM MODEL

We consider a TH binary phase shift keying (BPSK) UWB system. The k th user's signal can be described as [1]

$$s^{(k)}(t) = \sqrt{\frac{E_b}{N_s}} \sum_{j=-\infty}^{+\infty} d_{\lfloor j/N_s \rfloor}^{(k)} p\left(t - jT_f - c_j^{(k)}T_c\right) \quad (1)$$

where E_b is the bit energy, and N_s is the number of frames in an information bit. The random variable (RV) $d_{\lfloor j/N_s \rfloor}^{(k)}$ is the $\lfloor j/N_s \rfloor$ th information bit in the j th frame of the k th user, which takes value from $\{+1, -1\}$ with equal probability. $\lfloor \cdot \rfloor$ is the flooring operator. $p(t)$ is the signal pulse with width T_p , and is normalized so that $\int_{-\infty}^{+\infty} p^2(t)dt = 1$. T_f is the time duration of a frame, thus the bit duration $T_b = N_s T_f$. $\{c_j^{(k)}\}$ represents the TH code for the k th user. It is pseudorandom and its element takes an integer value from $[0, N_h)$. Here N_h is the number of hops per frame. T_c is the hop width satisfying the condition $N_h T_c \leq T_f$.

Assuming that N_u users are transmitting, then the received signal is

$$r(t) = \sum_{k=1}^{N_u} A_k s^{(k)}(t - \tau_k) + n(t) \quad (2)$$

where A_k and τ_k is the channel gain and propagation delay of the k th user respectively. Following a widely adopted assumption, $\{\tau_k\}_{k=1}^{N_u}$ are assumed to be uniformly distributed on bit duration $[0, T_b]$ [10]. $n(t)$ is an additive white Gaussian noise (AWGN) process with two-sided power spectral density $N_0/2$.

Consider using a correlation receiver to coherently demodulate the desired user's signal. Assume the first user is the desired user and $d_0^{(1)}$ is the desired symbol. Without loss of generality, we assume that $c_j^{(1)}$ representing the TH sequence for the desired user is 0, for all j [13]. Assuming perfect synchronization, $p(t - \tau_1 - mT_f)$ is correlation waveform. The detection of desired symbol $d_0^{(1)}$ is based on the N_s

outputs of the correlator in bit duration. The correlator output in the m th frame of $d_0^{(1)}$ ($0 \leq m < N_s$) is given by

$$R_m = \int_{mT_f + \tau_1}^{(m+1)T_f + \tau_1} r(t)p(t - \tau_1 - mT_f)dt = S_m + N_m + I_m = S_m + Y_m \quad (3)$$

where $S_m = A_1 \sqrt{E_b/N_s} d_0^{(1)}$ is the desired signal component, and N_m is the AWGN component which is Gaussian distributed with zero mean and variance $N_0/2$. I_m is the interference term and can be written as the following with the assumption $N_h T_c < T_f/2 - 2T_p$ [1]

$$I_m = \sqrt{\frac{E_b}{N_s}} \sum_{k=2}^{N_u} A_k d_{\lfloor (m+m_k)/N_s \rfloor}^{(k)} R\left(\alpha_k - c_{m+m_k}^{(k)} T_c\right) \quad (4)$$

where $R(x)$ is the autocorrelation function of the pulse $p(t)$; m_k is the value of the time difference $\tau_1 - \tau_k$ rounded to the nearest frame time, and α_k is the fractional part of time difference [10]. Note that when the pulse of the desired user in the m th frame is not collided by interfering pulse I_m equals to 0, and when it is collided by one or more interfering pulses I_m is a RV. The RV $Y_m = I_m + N_m$ is the total disturbance in the m th frame.

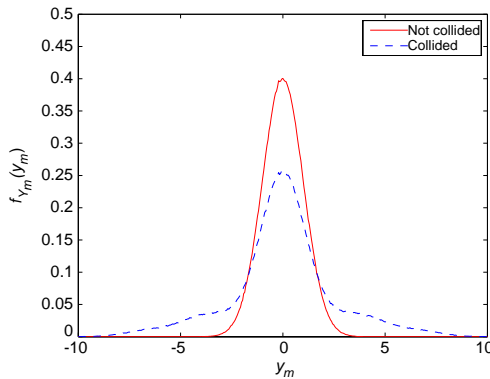
3. DISTRIBUTION APPROXIMATION OF THE TOTAL DISTURBANCE

The distribution of the total disturbance in a single frame which contains AWGN and MUI when the received pulse is collided by interfering pulses may be quite different from that when the received pulse is not collided since the total disturbance in this case contains only AWGN. To evaluate this difference, we simulate a TH-UWB communication system with multiple users. In this simulation (also other simulations in this paper), the second-order Gaussian monocycle $p(t) = [1 - 4\pi(t/\tau_p)^2] \exp[-2\pi(t/\tau_p)^2]$ is used as the signal pulse where τ_p is the time normalization factor [13]. The parameter settings are listed in Table 1 following [10, 13]. Based on whether the pulse of the desired user is collided or not, the samples of Y_m obtained in the simulation are grouped into two sets.

Figure 1 represents the simulated PDF of the amplitude of Y_m when the pulse of the desired user is not collided and that when the pulse of the desired user is collided. The simulated PDFs are acquired by histogram and the bin width is 0.05. There are 2×10^6 samples generated to obtain each simulated PDF. It can be observed that the distribution of Y_m when the pulse of the desired user is not collided and

Table 1. Parameters of the TH-BPSK UWB system.

Parameter	Notation	Value
Time normalization factor [ns]	τ_p	0.2877
Impulse width [ns]	T_p	0.7
Frame duration [ns]	T_f	20
Hop width [ns]	T_c	0.9
Number of hops per frame	N_h	8
Number of frames per bit	N_s	4
Number of users	N_u	4
Channel gain of interfering users	$\{A_k\}_{k=2}^{N_u}$	1
Signal-to-noise ratio [dB]	$\text{SNR} = E_b/N_0$	20

**Figure 1.** The simulated PDF of the amplitude of Y_m .

that when the pulse of the desired user is collided are different. Owing to the obvious discrepancy, one single PDF could not well approximate the distribution of Y_m simultaneously for the two cases above.

In this paper we use two separated approximating (SA) PDFs to model the distribution of Y_m . It can be modeled as a Gaussian PDF when the pulse of the desired user is not collided since Y_m contains only Gaussian noise. When the pulse of the desired user is collided Y_m consists of MUI and Gaussian noise, and a generalized Gaussian PDF is adopted to approximate the distribution of Y_m . As Gaussian

model is a special case of generalized Gaussian model, the generalized Gaussian PDF with different values of the parameters is adopted to model the distribution of Y_m for the collided and not collided cases, and it can be written as [23]

$$f_{Y_m}(y_m) = \frac{1}{2\Gamma(1 + 1/p)A(p, \sigma)} \exp \left[- \left| \frac{y_m - \mu}{A(p, \sigma)} \right|^p \right] \quad (5)$$

where $\Gamma(z)$ is the Gamma function given by

$$\Gamma(z) = \int_0^{\infty} \exp(-t) \cdot t^{z-1} dt \quad (6)$$

and

$$A(p, \sigma) = \sigma [\Gamma(1/p)/\Gamma(3/p)]^{1/2}. \quad (7)$$

μ , σ , p are, respectively, the mean, standard deviation and shape parameter of the distribution [24]. When the pulse of the desired user is not collided, we have $\mu = 0$ and $\sigma^2 = N_0/2$, thus the SA PDF $f_{Y_m}(y_m)$ is denoted as $f_{Y_m}^a(y_m)$, and can be written as

$$f_{Y_m}^a(y_m) = \frac{1}{\sqrt{2\pi\sigma^2}} \exp \left[- \frac{(y_m - \mu)^2}{2\sigma^2} \right]. \quad (8)$$

When the pulse of the desired user is collided, the SA PDF $f_{Y_m}(y_m)$ is denoted as $f_{Y_m}^b(y_m)$. The parameters μ , σ , p in $f_{Y_m}^b(y_m)$ are estimated by calculating the mean, second moment and kurtosis of Y_m when the pulse is collided using the system parameters, and the derivation is provided in the appendix.

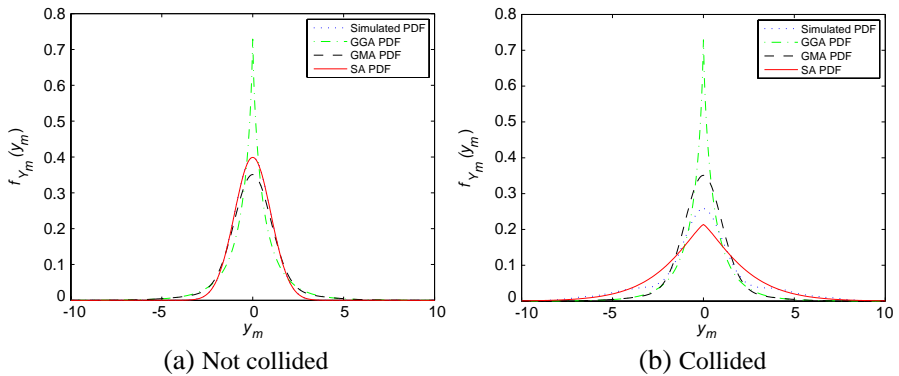
In Figure 2 the SA PDFs are plotted with the simulated PDFs when the pulse of the desired user is not collided and when it is collided, and in addition the Gaussian mixture approximating (GMA) PDF [12] and the generalized Gaussian approximating (GGA) PDF [13] are also presented. The parameter settings adopted are the same as those given in Table 1. It can be seen that when the pulse of the desired user is not collided, the SA PDF $f_{Y_m}^a(y_m)$ provides excellent match to the simulated PDF, and when the pulse of the desired user is collided, the SA PDF $f_{Y_m}^b(y_m)$ also provides good approximation to the simulated PDF.

To evaluate PDF approximation, the Kullback-Leibler (K-L) distance is introduced to characterize the similarity between the simulated PDF and approximating PDF [25]. The K-L distance between PDFs $f_{X_1}(x)$ and $f_{X_2}(x)$ is given by

$$KL[f_{X_1}(x), f_{X_2}(x)] = \int_{-\infty}^{+\infty} f_{X_1}(x) \ln \frac{f_{X_1}(x)}{f_{X_2}(x)} dx. \quad (9)$$

Table 2. *KLS* between the simulated PDF and the approximating PDFs.

Approximating PDFs	Not collided	Collided
GGA PDF	0.349	0.410
GMA PDF	0.256	0.333
SA PDF	0.005	0.069

**Figure 2.** (a) The simulated PDF, the SA PDF $f_{Y_m}^a(y_m)$, the GMA PDF and the GGA PDF when the pulse of the desired user is not collided. (b) The simulated PDF, the SA PDF $f_{Y_m}^b(y_m)$, the GMA PDF and the GGA PDF when the pulse of the desired user is collided.

The smaller the K-L distance, the more would be the similarity between the two PDFs. As the K-L distance metric is asymmetric, the sum of the two K-L distances $KLS[f_{X_1}(x), f_{X_2}(x)] = KL[f_{X_1}(x), f_{X_2}(x)] + KL[f_{X_2}(x), f_{X_1}(x)]$ is adopted to evaluate the similarity between the simulated PDF and approximating PDF. The *KLS* between the simulated PDF and the approximating PDFs plotted in Figure 2(a) and Figure 2(b) are listed in Table 2. Obviously, for the two cases, the SA PDF has a smaller distance to the simulated PDF than the GGA PDF and the GMA PDF, especially when the pulse of the desired user is not collided. Then it can be verified that the two generalized Gaussian PDFs with different values of parameters better approximate the distribution of the total disturbance than the approximating generalized Gaussian PDF and Gaussian mixture PDF.

4. DETECTION SCHEME

Using the two SA PDFs, the new detection scheme of TH-UWB receiver is proposed based on the maximum likelihood (ML) method. With the assumption that the total disturbance terms are independent in different frames of a bit [12], the final decision statistic for the ML method can be expressed as follows [26]

$$U = \log \prod_{m=0}^{N_s-1} \frac{f_{Y_m}(R_m - |S_m|)}{f_{Y_m}(R_m + |S_m|)} = \sum_{m=0}^{N_s-1} Z_m \quad (10)$$

where $f_{Y_m}(\cdot)$ is the PDF of Y_m , and Z_m is the log-likelihood ratio in the m th frame, which is given by

$$Z_m = \log \frac{f_{Y_m}(R_m - |S_m|)}{f_{Y_m}(R_m + |S_m|)}. \quad (11)$$

When the pulse of the desired user in the m th frame is not collided, we use $f_{Y_m}^a(y_m)$ to model the distribution of the total disturbance in this frame, and then the log-likelihood ratio in the m th frame is calculated according to (11). When the pulse of the desired user in the m th frame is collided, we use $f_{Y_m}^b(y_m)$ to model the distribution of the total disturbance in this frame, and the log-likelihood ratio in the m th frame can be obtained accordingly. Using the final decision statistic, the transmitted information bit $d_0^{(1)}$ is detected according to the rule

$$U > 0 \Rightarrow d_0^{(1)} = +1 \quad (12)$$

$$U < 0 \Rightarrow d_0^{(1)} = -1. \quad (13)$$

If $U = 0$, $d_0^{(1)}$ is decided by a fair coin toss.

5. SIMULATION RESULTS AND DISCUSSION

In this section, we compare the BER performance of the proposed receiver with that of the blinking receiver, the GM receiver, the p-order receiver and the CMF receiver through simulation. The parameter settings are the same as those given in Table 1. When demonstrating the BER as a function of one parameter, other system parameter settings will be specified and fixed.

Figure 3 shows the BER of the receivers as a function of the SNR. It can be seen that when SNR is small the proposed receiver achieves about the same BER as the other receivers, and when we increase SNR it outperforms other receivers. When SNR exceeds 25 dB the BER of the proposed receiver is approaching its error floor which is two orders

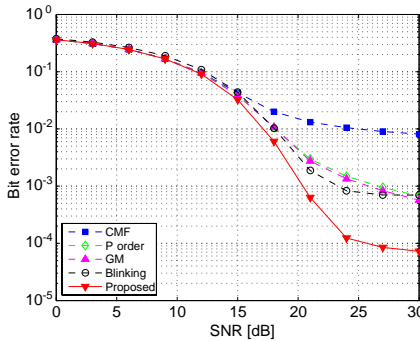


Figure 3. The BER versus SNR for the proposed receiver, the blinking receiver, the GM receiver, the p-order receiver and the CMF receiver. The channel gain of the desired user is 0.25.

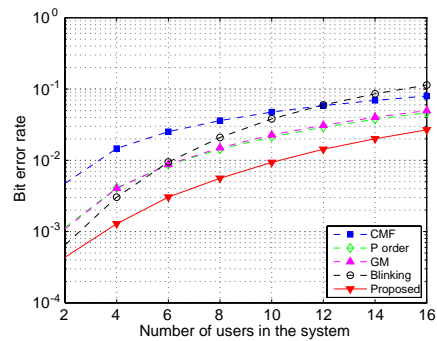


Figure 4. The BER versus number of users in the system for the proposed receiver, the blinking receiver, the GM receiver, the p-order receiver and the CMF receiver. The channel gain of the desired user is 0.25 and SNR = 20 dB.

lower than that of CMF receiver and one order lower than that of the other receivers.

The observations can be explained as follows. For small values of SNR, the AWGN dominates the MUI, and then the difference between the distribution of the total disturbance when the received pulse is collided and that when the received pulse is not collided is small. In this case, one PDF is sufficient for the distribution approximation of the total disturbance, so the proposed receiver achieves almost the same BER of the GM receiver, the p-order receiver and the CMF receiver. For large values of SNR, the MUI dominates the AWGN, and then the distribution of the total disturbance when the received pulse is collided differs significantly from that when the received pulse is not collided. The distribution of the total disturbance can not be well approximated by one PDF; therefore, the proposed receiver based on two PDFs outperforms the other three receivers. The proposed receiver outperforms the blinking receiver by taking the collided pulses into account instead of discarding them, and as the SNR grows, the desired signal component is more and more significant, thus the BER improvement achieved by the proposed receiver over the blinking receiver increases as the SNR grows.

Figure 4 shows the BER of the receivers as a function of the number of users in the system. It is shown that the proposed receiver

outperforms the other receivers for all the investigated values of the number of users in the system. When there are 8 users in the system the BER of proposed receiver is 5.8×10^{-3} while the lowest BER of other receivers is 1.5×10^{-2} . The reason of the BER improvement over the GM receiver, the p-order receiver and the CMF receiver is that the proposed receiver better models the total disturbance and the reason of BER improvement over the blinking receiver is that it does not discard the collided pulses.

It can also be seen that as the number of users increases, the BER performance gains achieved by the proposed receiver over the p-order receiver, the GM receiver and the CMF receiver decrease. The reason is that the proposed receiver perfectly models the distribution of Y_m only when the pulse of the desired user is not collided. As the number of users increases, the pulses of the desired user are collided more frequently, and then the proposed receiver less frequently models the distribution of Y_m perfectly, thus the BER gains decrease. It can also be observed that as the number of users increases, the BER performance gain achieved by the proposed receiver over the blinking receiver increases. The reason is that as the number of users increases, the blinking receiver discards more collided pulses owing to the increased pulse collision probability while the proposed receiver does not discard any pulse.

Figure 5 shows the BER of the receivers as a function of the channel gain of the desired user. It is shown that the proposed receiver outperforms the other receivers for most investigated values of the channel gain of the desired user as the proposed receiver does not discard the collided pulses and better models the total disturbance.

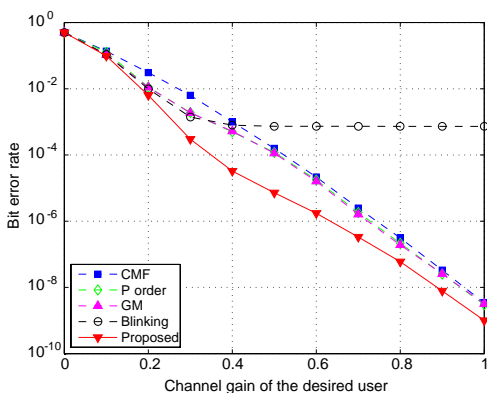


Figure 5. The BER versus channel gain of the desired user for the proposed receiver, the blinking receiver, the GM receiver, the p-order receiver and the CMF receiver.

When A_1 is 0.5, the BER of proposed receiver is 7.3×10^{-6} , which is more than one order lower than the lowest BER of the other receivers. It can be seen that the proposed receiver achieves almost the same BER performance as the other receivers when A_1 (the channel gain of the desired user) is smaller than 0.1. The reason is that when A_1 is small, the desired signal component is small, and then all the receivers achieve very high BER, thus the difference among them is small. It can also be found that when A_1 is larger than a threshold, about 0.4, the BER performance gains achieved by the proposed receiver over the GM receiver, the p-order receiver and the CMF receiver decrease as A_1 increases. The reason is that when A_1 is large enough, the receivers above can all achieve low BER due to the large desired signal component, and then the modeling of the total disturbance does not significantly impact the BER.

Note that the slope of the BER curve of the proposed receiver is changed when the channel gain exceeds about 0.4. It can be explained as follows. When the received pulse is not collided the BER of the receiver decreases slowly with the increase of A_1 at large A_1 since the BER curve achieves error floor. When the received pulse is collided the BER of the receiver decreases at the same pace for the whole the range of A_1 considered since the total power of the multiuser interference plus noise is too high to achieve the error floor for large A_1 . In summary the overall BER for both cases, when the received pulse is collided and when it is not, decreases slower with the increase of A_1 when A_1 is large than when it is small.

It is also shown that when A_1 is large the BER of the blinking receiver does not decrease as A_1 increases while the BER of the proposed receiver keeps decreasing. For the blinking receiver, when A_1 is large enough the BER of the bits in which at least one pulse is not collided is approaching to zero while the BER of the bits in which all the pulses are collided is 50% which is independent of A_1 since the signal detection decision at this time is made by a fair coin toss. Therefore there is a lower bound of the BER performance of blinking receiver when A_1 is large, which is determined by the collision probability. But there is not such a bound for the proposed receiver.

6. CONCLUSION

In this paper, a novel TH-UWB receiver is proposed based on two PDFs approximation in multiuser systems. We use two PDFs to approximate the distribution of the total disturbance when the pulse of the desired user is collided and also when it is not collided respectively. A new detection scheme is proposed based on the two PDFs. Simulation

results show that the novel receiver achieves better BER performance than blinking receiver, GM receiver, p-order receiver and CMF receiver at different values of the SNR, the number of the users and the channel gain of the desired user. It is revealed that taking whether or not the received pulses are collided into consideration allows a better design of UWB receivers.

The objective of this paper is to design a new receiver which can be applied in outdoor environments where wireless channel can be modeled as single path. It is our future work to extend the proposed receiver in a multipath environment where a pulse collision detection module will be developed and can be conducted on each receiver without control channels.

ACKNOWLEDGMENT

The work was supported by the Program for New Century Excellent Talents in University (NCET) and the State Key Laboratory of Wireless Mobile Communications (CATT), National Natural Science Foundation of China under Grant No. 61231013 and National Basic Research Program (973 Program) under Grant No. 2010CB731800. The authors thank the editors and anonymous reviewers for their valuable comments that have helped to improve the paper.

APPENDIX A.

In this appendix, the derivation of the parameters in $f_{Y_m}^b(y_m)$ is provided. $f_{Y_m}^b(y_m)$ is rewritten as follows

$$f_{Y_m}^b(y_m) = \frac{1}{2\Gamma(1 + 1/p)A(p, \sigma)} \exp \left[- \left| \frac{y_m - \mu}{A(p, \sigma)} \right|^p \right] \quad (\text{A1})$$

where μ , σ , p are, respectively, the mean, standard deviation and shape parameter to be estimated. The function $A(p, \sigma) = \sigma[\Gamma(1/p)/\Gamma(3/p)]^{1/2}$ is the scaling factor and $\Gamma(\cdot)$ is the Gamma function.

We let J_m denote the MUI component in the m th frame when the pulse of the desired user in this frame is collided by interfering pulse. Then when the pulse of the desired user in the m th frame is collided, the total disturbance in this frame is given by

$$Y_m = N_m + J_m. \quad (\text{A2})$$

μ is estimated by calculating the mean of Y_m . As N_m and J_m are independent and both have zero means, the estimated value for μ is

given by

$$\hat{\mu} = E[Y_m] = E[N_m] + E[J_m] = 0. \quad (\text{A3})$$

σ is estimated by calculating the second central moment of Y_m , which has the form $E[Y_m^2] = E[N_m^2] + E[J_m^2]$. The second central moment of J_m is given by

$$E[J_m^2] = E[I_m^2]/\varepsilon \quad (\text{A4})$$

where $\varepsilon = 1 - (1 - 2T_p/T_f)^{N_u-1}$ and $E[I_m^2] = \frac{E_b(N_u-1)A_k^2}{N_s T_f} \int_{-\infty}^{+\infty} R^2(x) dx$ [12].

The variance of the AWGN component in the m th frame $E[N_m^2] = N_0/2$, and then the estimated value for σ is given by

$$\hat{\sigma} = \sqrt{E[Y_m^2]} = \sqrt{\frac{N_0}{2} + \frac{E_b(N_u-1)A_k^2}{N_s T_f \varepsilon} \int_{-\infty}^{+\infty} R^2(x) dx}. \quad (\text{A5})$$

p is estimated by kurtosis matching method. The kurtosis of Y_m is expressed as

$$k(p) = \frac{E[Y_m^4]}{(E[Y_m^2])^2} - 3 = \frac{\Gamma(1/p)\Gamma(5/p)}{\Gamma^2(3/p)} - 3. \quad (\text{A6})$$

The fourth central moment of Y_m is given by

$$E[Y_m^4] = E[J_m^4] + 6E[J_m^2]E[N_m^2] + E[N_m^4]. \quad (\text{A7})$$

As the PDF of I_m has the form [12]

$$f_{I_m}(i_m) = (1 - \varepsilon)\delta(i_m) + \varepsilon f_{J_m}(j_m), \quad (\text{A8})$$

we have

$$E[J_m^4] = E[I_m^4]/\varepsilon \quad (\text{A9})$$

where $E[I_m^4] = \left(\frac{E_b}{N_s}\right)^2 A_k^4 \left[\frac{N_u-1}{T_f} \int_{-\infty}^{+\infty} R^4(x) dx + \frac{6}{T_f^2} C_{N_u-1}^2 \left[\int_{-\infty}^{+\infty} R^2(x) dx\right]^2\right]$ [13].

The fourth moment of the AWGN component in the m th frame $E[N_m^4] = 3N_0^2/4$. Then the estimated value for the shape parameter, \hat{p} , satisfies

$$\frac{\Gamma(1/\hat{p})\Gamma(5/\hat{p})}{\Gamma^2(3/\hat{p})} = \frac{E[J_m^4] + 6E[J_m^2]E[N_m^2] + E[N_m^4]}{(E[J_m^2] + E[N_m^2])^2}. \quad (\text{A10})$$

REFERENCES

1. Win, M. Z. and R. A. Scholtz, "Ultra-wide bandwidth time-hopping spread-spectrum impulse radio for wireless multiple-access communications," *IEEE Trans. Commun.*, Vol. 48, No. 4, 679–691, 2000.

2. Beaulieu, N. C. and D. J. Young, "Designing time-hopping ultrawide bandwidth receivers for multiuser interference environments," *Proc. IEEE*, Vol. 97, No. 2, 255–284, 2009.
3. Gao, A.-M., Q. H. Xu, H.-L. Peng, W. Jiang, and Y. Jiang, "Performance evaluation of UWB on-body communication under WiMAX off-body EMI existence," *Progress In Electromagnetics Research*, Vol. 132, 479–498, 2012.
4. Zhang, Z. and Y. H. Lee, "A robust CAD tool for integrated design of UWB antenna system," *Progress In Electromagnetics Research*, Vol. 112, 441–457, 2011.
5. Liu, J. Q., K. J. Song, and Y. Fan, "UWB BPF with triple notched bands using novel dual-mode SIR and asymmetrical coupling structure," *Journal of Electromagnetic Waves and Applications*, Vol. 26, No. 16, 2112–2120, 2012.
6. Lizzi, L., G. Oliveri, and A. Massa, "A time-domain approach to the synthesis of UWB antenna systems," *Progress In Electromagnetics Research*, Vol. 122, 557–575, 2012.
7. Tang, H.-Y., P. Zhuo, X.-L. Gao, F.-F. Zhao, and L.-W. Li, "Compact planar UWB antenna with triple band-notched characteristics for WIMAX/WLAN/ITU bands," *Journal of Electromagnetic Waves and Applications*, Vol. 26, No. 14, 1873–1880, 2012.
8. Lie, J. P., B. P. Ng, and C. M. S. See, "Multiple UWB emitters DOA estimation employing time hopping spread spectrum," *Progress In Electromagnetics Research*, Vol. 78, 83–101, 2008.
9. Liu, X.-F., B.-Z. Wang, S.-Q. Xiao, and J. H. Deng, "Performance of impulse radio UWB communications based on time reversal technique," *Progress In Electromagnetics Research*, Vol. 79, 401–413, 2008.
10. Beaulieu, N. C. and B. Hu, "Soft-limiting receiver structures for time-hopping UWB in multiple-access interference," *IEEE Trans. Veh. Technol.*, Vol. 57, No. 2, 810–818, 2008.
11. Hu, B. and N. C. Beaulieu, "Accurate evaluation of multiple-access performance in TH-PPM and TH-BPSK UWB systems," *IEEE Trans. Commun.*, Vol. 52, No. 10, 1758–1766, 2004.
12. Ghasemi, A. and S. Nader-Esfahani, "Nonlinear pulse combining in impulse radio UWB systems," *IET Commun.*, Vol. 1, No. 6, 1289–1295, 2007.
13. Beaulieu, N. C., H. Shao, and J. Fiorina, "P-order metric UWB receiver structures with superior performance," *IEEE Trans. Commun.*, Vol. 56, No. 10, 1666–1676, 2008.

14. Fishler, E. and H. V. Poor, "Low-complexity multiuser detectors for time-hopping impulse-radio systems," *IEEE Trans. Signal Process.*, Vol. 52, No. 9, 2561–2571, 2004.
15. Hosseini, I. and N. C. Beaulieu, "Optimal error rate performance of binary TH-UWB receivers in multiuser interference," *Proc. IEEE GLOBECOM' 2008*, New Orleans, US, 2008.
16. Chen, Z. and Y.-P. Zhang, "Effects of antennas and propagation channels on synchronization performance of a pulse-based ultra-wideband radio system," *Progress In Electromagnetics Research*, Vol. 115, 95–112, 2011.
17. Mabrouk, I. B., L. Talbi, M. Nedil, and K. Hettak, "The effect of the human body on MIMO-UWB signal propagation in an underground mine gallery," *Journal of Electromagnetic Waves and Applications*, Vol. 26, No. 4, 560–569, 2012.
18. Videv, S., H. Haas, J. S. Thompson, and P. M. Grant, "Energy efficient resource allocation in wireless systems with control channel overhead," *Proc. IEEE WCNCW' 2012*, Edinburgh, UK, 2012.
19. Doerr, C., D. Grunwald, and D. C. Sicker, "Dynamic control channel management in presence of spectrum heterogeneity," *Proc. IEEE MILCOM' 2008*, Boulder, US, 2008.
20. Guvenc, I., Z. Sahinoglu, and P. V. Orlik, "TOA estimation for IR-UWB systems with different transceiver types," *IEEE Trans. Microw. Theory Tech.*, Vol. 52, No. 4, 1876–1886, 2006.
21. Ahmed, Q. Z. and L.-L. Yang, "Reduced-rank adaptive multiuser detection in hybrid direct-sequence time-hopping ultrawide bandwidth systems," *IEEE Trans. Wirel. Commun.*, Vol. 9, No. 1, 156–167, 2010.
22. Guvenc, I. and H. Arslan, "A review on multiple access interference cancellation and avoidance for IR-UWB," *Signal Process.*, Vol. 87, No. 4, 623–653, 2007.
23. Gradshteyn, I. S. and I. M. Ryzhik, *Table of Integrals, Series, and Products*, Academic Press, Inc., Massachusetts, 1994.
24. Kay, S. M., *Fundamentals of Statistical Signal Processing: Detection Theory*, Prentice Hall, New Jersey, 1998.
25. Guvenc, I., H. Arslan, S. Gezici, and H. Kobayashi, "Adaptation of two types of processing gains for UWB impulse radio wireless sensor networks," *IET Commun.*, Vol. 1, No. 6, 1280–1288, 2007.
26. Proakis, J. G., *Digital Communications*, McGraw Hill, New York, 2001.